ISMIP — HOM

ICE SHEET MODEL INTERCOMPARISON PROJECT

Benchmark experiments for numerical Higher-Order ice-sheet Models

Frank PATTYN[1]
Laboratoire de Glaciologie
Université Libre de Bruxelles
Belgium

Tony PAYNE[2]
School of Geographical Sciences
University of Bristol
England

February 28, 2006

[1]Laboratoire de Glaciologie, Département des Sciences de la Terre et de l'Environnement (DSTE), Université Libre de Bruxelles, Av. F. Roosevelt 50, B-1050 Brussels, Belgium (email: fpattyn@ulb.ac.be)

[2]Centre for Polar Observation and Modelling, School of Geographical Sciences, University of Bristol, Bristol B88 1SS, England (email: a.j.payne@bristol.ac.uk)

Contents

1 Introduction

The tests proposed below were defined and partly discussed during the *International Symposium on Physical and Mechanical Processes in Ice in relation to Glacier and Ice-sheet Modelling*, held in Chamonix Mont-Blanc, France, 26–30 August 2002 and during a first coordination meeting, held in Brussels, Belgium, June 3 and 4, 2003. The purpose of these tests is to fix benchmarks for future modelling attempts and to detect eventual weaknesses in numerical approaches of higher-order models. The experiments may be somewhat restrictive and may not be appropriate for all kinds of models.

During former model intercomparison exercises (EISMINT 1 and 2), a number of benchmarks were proposed for ice sheet models as well as for ice shelf models. The bulk of these ice-sheet models were based on the so-called *shallow-ice approximation* (SIA). In this exercise we will focus on so-called higher-order models, i.e. models that incorporate further mechanical effects, principally longitudinal stress gradients, or the full Stokes system. With longitudinal stresses we basically mean all stress components apart from the two horizontal plane shear components (Hindmarsh, 2004).

We tried to make the experiments accessible for many types of models, i.e. flowline models, vertically integrated planform models, as well as full three-dimensional models. The experiments are valid for both finite difference (FD) and finite element (FE) models. Furthermore, the grid type (regular or not) is unimportant.

With exception of experiment F, all experiments are diagnostic, i.e. time evolution is not considered. This means that for a given geometry of the ice mass, a Glen-type flow law, and given appropriate boundary conditions, the stress and velocity field can be calculated. Experiment F considers time-dependent response (the experiment is run until the free surface and velocity field reach a steady state) for a constant viscosity (linear flow law). For this experiment analytical solutions exists that are developed by Gudmundsson (2003).

All thermomechanical effects are neglected and an isotherm ice mass is considered. Experiments include ideal geometry tests as well as a real case experiment on Haut Glacier d'Arolla. The experiments are designed for the following types of higher-order models:

3D models: HHVF and HHVC, i.e. 2 horizontal dimensions and one vertical dimension. F = FULL (first, second-order, or solution of the full Stokes equations); C = CHANNEL (only solution for horizontal velocity v_x in the direction of the ice flow x). For C-type models, the stress field should include both vertical shear τ_{xz} as

well as longitudinal stresses τ_{xx} and their gradients. F-type models also include τ_{yz}, τ_{yy} and τ_{xy} (higher-order models). All stress gradients are included in the full Stokes models.

2D planform models: HHF, i.e. 2 horizontal dimensions but integrated over the vertical. These models are basically ice-shelf models, but should be extended with a friction coefficient so that ice-stream flow can be simulated as well (so-called shelfy-stream model, e.g. MacAyeal, 1993).

2D flowline models: HVF and HVC, i.e. one horizontal dimension (in the direction of the ice flow) and one vertical dimension. The stress field should include both vertical shear τ_{xz} as well as longitudinal stresses τ_{xx}. The models considered are flowline models (HVF) which eventually include a parameterization of the width of the flowline, or channel models (HVC).

The diagnostic experiments are divided into three groups. Experiments A–B are based on ice-sheet flow and focus on the ice flow over a bumpy and rippled bed on varying spatial scales; experiments C–D focus on ice stream flow, with a varying basal friction; experiment E is an application to the Haut Glacier d'Arolla geometry; experiment F is the time-dependent response of the ice flow over a Gaussian bump with a linear flow law. Table I lists the type of models that can participate in each of the model experiments.

Experiment	**Model type**
A	HHVF, HHVC
B	HHVF, HHVC, HVF, HVC
C	HHVF, HHVC, HHF
D	HHVF, HHVC, HHF, HVF, HVC
E	HVF, HVC, HHVF, HHVC
F	HHVF, HHVC

Table I: *Model type versus experiment.*

2 General model setup

2.1 Model physics, parameters and constants

A higher-order model is any type of ice sheet or glacier model that incorporates further mechanical effects, principally longitudinal stress gradients. With longitudinal stresses we basically mean all stress components apart from the two horizontal plane shear components (Hindmarsh, 2004). Such models are based on conservation laws of mass and momentum, i.e.

$$\nabla \cdot \vec{\mathbf{v}} = 0\,, \tag{1}$$

$$\rho \frac{\mathrm{d}\vec{\mathbf{v}}}{\mathrm{d}t} = \nabla \cdot \sigma + \rho \vec{\mathbf{g}}\,, \tag{2}$$

where ρ is the ice density, $\vec{\mathbf{g}}$ gravitational acceleration, $\vec{\mathbf{v}}$ the velocity vector, and $[\sigma]$ the stress tensor. Values for parameters and constants are given in Table II. Generally, acceleration terms in (2) are neglected and gravitational acceleration is considered only important in the vertical direction, so that the linear momentum becomes

$$\frac{\partial \sigma_{xx}}{\partial x} + \frac{\partial \sigma_{xy}}{\partial y} + \frac{\partial \sigma_{xz}}{\partial z} = 0\,, \tag{3}$$

$$\frac{\partial \sigma_{yx}}{\partial x} + \frac{\partial \sigma_{yy}}{\partial y} + \frac{\partial \sigma_{yz}}{\partial z} = 0\,, \tag{4}$$

$$\frac{\partial \sigma_{zx}}{\partial x} + \frac{\partial \sigma_{zy}}{\partial y} + \frac{\partial \sigma_{zz}}{\partial z} = \rho g\,. \tag{5}$$

Solving (3) – (5) leads to the full Stokes solution. In higher-order models some simplifications are made to the above system of equations. All models that take part in the intercomparison should use Glen's flow law, which relates strain rates to stresses by

$$\dot{\varepsilon}_{ij} = A \tau_e^{n-1} \tau_{ij} \tag{6}$$

where $\dot{\varepsilon}_{ij}$ is the strain rate component, A the flow parameter, τ_e the effective stress (or the second invariant of the stress tensor), and τ_{ij} the deviatoric stress component. Written in terms of effective viscosity η this gives

$$\tau_{ij} = 2\eta\, \dot{\varepsilon}_{ij}, \quad \eta = \frac{1}{2} A^{-1/n}\, \dot{\varepsilon}_e^{(1-n)/n} \tag{7}$$

where $\dot{\varepsilon}_e$ is the effective strain (or the second invariant of the strain-rate tensor). In some models the flow parameter A is defined by its inverse $B = A^{-1/n}$. Since only isotherm experiments are considered, the value for A is taken constant for the whole ice mass.

Symbol	Constant	Value	Units
A	Ice-flow parameter	10^{-16}	Pa^{-n} a^{-1}
ρ	Ice density	910	kg m^{-3}
g	Gravitational constant	9.81	m s^{-2}
n	Exponent in Glen's flow law	3	
	Seconds per year	31 556 926	s a^{-1}

Table II: *Constants for the numerical model.*

2.1.1 Isotropic and hydrostatic pressure

Basic output for the model experiments is the velocity field, at the surface and at the base, the latter only for experiments C and D. Another model output is the difference between the isotropic and hydrostatic pressure at the bed, defined by

$$\Delta p = p_I - p_H = \frac{1}{3}(\sigma_{xx} + \sigma_{yy} + \sigma_{zz}) - p_H \tag{8}$$

The deviatoric normal stress is then defined as the full normal stress minus the isotropic pressure, or more general: $\tau_{ij} = \sigma_{ij} - p_I \delta_{ij}$, where δ_{ij} is the Kronecker delta ($\delta_{ij} = 1$ if $i = j$, and $\delta_{ij} = 0$ if $i \neq j$). The hydrostatic pressure is defined as $p_H = \sigma_{xx} = \sigma_{yy} = \sigma_{zz} = -\rho g H$. For the *shallow-ice approximation*, the isotropic pressure at the bed equals the hydrostatic pressure, or $p_I = p_H$, so that Δp = 0.

2.1.2 Basal drag, β^2 and basal shear stress

The friction coefficient β^2 is used to introduce basal sliding in the model. By definition, zero friction at the base means that the sum of all stress components equals zero, i.e. the basal surface is stress free. Such conditions exist at the base of an ice shelf where the ocean water does not exert significant friction. The stress-free condition also holds at the surface of the ice mass (contact with air). On the contrary, when ice is frozen to the bedrock, friction becomes infinitely large and hence no sliding occurs. The friction parameter is related to the basal drag τ_b (sum of all basal resistance at the base) and the basal velocity by

$$\tau_{\mathbf{b}} = \mathbf{v_b}\beta^2 \tag{9}$$

where $\mathbf{v_b}$ is the basal velocity. β^2 (Pa a m^{-1}) is a scalar quantity and always positive (MacAyeal, 1993).

The basal shear stress components ($\tau_{xz}(z_b)$, $\tau_{yz}(z_b)$) must be calculated as well and form part of the output of the model results. They are also defined by

$$\tau_{xz}(z_b) = 2\eta(z_b)\,\dot{\varepsilon}_{xz}(z_b) = \eta(z_b)\left(\frac{\partial v_x(z_b)}{\partial z} + \frac{\partial v_z(z_b)}{\partial x}\right) \tag{10}$$

$$\tau_{yz}(z_b) = 2\eta(z_b)\,\dot{\varepsilon}_{yz}(z_b) = \eta(z_b)\left(\frac{\partial v_y(z_b)}{\partial z} + \frac{\partial v_z(z_b)}{\partial y}\right) \tag{11}$$

2.2 Boundary conditions

The theoretical experiments are designed in such a way that variations in bed topography or basal friction coefficient are periodic, so that periodic boundary conditions to the velocity field apply (for implementing periodic boundary conditions, see section 2.3.1). For experiments A–B, ice is considered frozen to the bed, which implies that $\mathbf{v}(z_b)$ = 0, z_b denoting the bed. Therefore, the friction coefficient β^2 is infinite everywhere on the domain (or at least *very* large). For experiments C–D, the friction coefficient β^2 is predefined, which will control the amount of basal sliding. Experiment E does not involve periodic boundary conditions, but is an application to an existing glacier geometry. Experiment F considers ice frozen to the bedrock and applies periodic boundary conditions.

2.2.1 Kinematic boundary conditions to the vertical velocity field

Kinematic boundary conditions apply to the vertical velocity field v_z. Since the bedrock is kept fixed in time and basal melting is neglected, the vertical velocity at the base of the ice mass is defined by

$$v_z(z_b) = v_x(z_b)\frac{\partial z_b}{\partial x} + v_y(z_b)\frac{\partial z_b}{\partial y} \tag{12}$$

where z_b is the bedrock elevation (lower boundary of the ice mass). Since the vertical velocity field must obey the incompressibility condition (1), and the surface accumulation/ablation is zero ($M(s)$ = 0), the vertical velocity at the surface contains the local imbalance as well and becomes a model output.

2.3 Model domain

The model domain is square. The minimum number of grid points is not predefined. It is advised that people use a discretization scheme for which they think that the best possible results are obtained. Since this might be model dependent, we allow everyone to choose the number of grid points in the horizontal as well as in the vertical direction. The basic parameter for the experiments is the length scale of the domain L, that applies to both horizontal directions. Experiments A–D are carried out for L = 160, 80, 40, 20, 10 and 5 km, respectively. A scaled horizontal distance is introduced for output, varying between 0 and 1,

$$\hat{x} = \frac{x}{L} \qquad \hat{y} = \frac{y}{L} \tag{13}$$

Finite element models may use any type of discretization scheme (a regular grid is not necessary), as long as the model domain length L is respected and periodic boundary conditions are implemented.

2.3.1 Periodic boundary conditions

Periodic boundary conditions are achieved by surrounding the simulation domain with an infinite number of copies of itself in the horizontal. To make this point clear, consider a finite difference grid, where the relation between the length scale and the grid resolution is given by

$$L = (N_x - 2) \cdot \Delta x \quad \text{or} \quad \Delta x = \frac{L}{N_x - 2} \tag{14}$$

Note that the last gridpoint N_x does not coincide with L. By doing so, velocities at the grid boundaries are defined by

$$\begin{aligned}
\mathbf{v}_{1,j,k} &= \mathbf{v}_{N_y-1,j,k} \\
\mathbf{v}_{N_y,j,k} &= \mathbf{v}_{2,j,k} \\
\mathbf{v}_{i,1,k} &= \mathbf{v}_{i,N_x-1,k} \\
\mathbf{v}_{i,N_x,k} &= \mathbf{v}_{i,2,k}
\end{aligned}$$

for $i = 1 \rightarrow N_y$, $j = 1 \rightarrow N_x$ and $k = 1 \rightarrow N_z$, where N_x, N_y, and N_z are the number of grid points in the x, y and z direction, respectively, and where $\mathbf{v}$ is any of the velocity

components (v_x, v_y, v_z). Defining the finite difference grid that way, $\hat{x}$ and $\hat{y}$ are related to the grid nodes as

$$\hat{x}_j = \frac{j-1}{N_x - 2} \qquad \hat{y}_i = \frac{i-1}{N_y - 2} \tag{15}$$

for $i = 1 \rightarrow N_y$, $j = 1 \rightarrow N_x$. Applying periodic boundary conditions is far from complicated and does not demand a lot of coding. Since any higher-order solution demands iterations, it is possible to add the periodic boundary conditions within one of these iterative loops. For the examples showed here on a finite difference grid, periodic boundary conditions were simply coded as follows (within the main iteration for the determination of the horizontal velocity field):

```
for (i = 1; i <= maxy; i++){
     for (k = 1; k <= nzeta; k++){
          uvel[i][1][k] = uvel[i][maxx - 1][k];
          vvel[i][1][k] = vvel[i][maxx - 1][k];
          uvel[i][maxx][k] = uvel[i][2][k];
          vvel[i][maxx][k] = vvel[i][2][k];
     }
}
for (j = 1; j <= maxx; j++){
     for (k = 1; k <= nzeta; k++){
          uvel[1][j][k] = uvel[maxy - 1][j][k];
          vvel[1][j][k] = vvel[maxy - 1][j][k];
          uvel[maxy][j][k] = uvel[2][j][k];
          vvel[maxy][j][k] = vvel[2][j][k];
     }
}
```

Nevertheless, we are aware that for certain people such coding exercise might be difficult. We therefore propose the following alternative: make the domain much larger, for instance $3 \times L$ by $3 \times L$, set the lateral boundary conditions as $\mathbf{v} = 0$, calculate the velocity field with the higher-order model and cut out the central part for display. Make sure that the central part of the model domain is not influenced by the choice of these lateral boundary conditions. If you think it is, enlarge the domain. The major drawback of such a setup is the higher computational cost and possible occurrence of numerical instabilities near the imposed boundaries.

All experiments described below were tested with a HHVF and a HVF model (Pattyn, 2002; Pattyn, 2003). The examples shown here are based on a grid of 41 by 41 grid points in both horizontal directions x and y, and 41 vertical layers in z. Horizontal grid-size for the shown experiment L = 80 is Δx = 2051.282051 m. These results should be regarded as illustrations, as the discretization scheme is not considered to be optimal.

3 Experiments

3.1 Experiment A: ice flow over a bumpy bed

3.1.1 Type of models

HHVF and HHVC

3.1.2 Description of the experiment

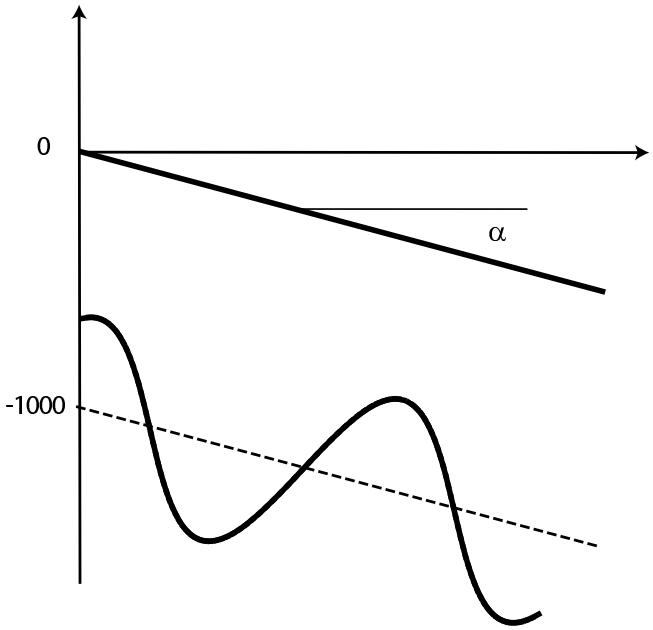

Figure 1: *Coordinate system for experiments A–D.*

Consider a parallel-sided slab of ice with a mean ice thickness H = 1000 m lying on a sloping bed with a mean slope $\alpha = 0.5^\circ$[1]. This slope is maximum in x and zero in y. The basal topography is then defined as a series of sinusoidal bumps with an amplitude of 500 m (Figure 1). The surface elevation is defined as

$$z_s(x,y) = -x \cdot \tan\alpha \tag{16}$$

where $\alpha = 0.5^\circ$. The basal topography is then given by

[1] $180^\circ = \pi$

$$z_b(x,y) = z_s(x,y) - 1000 + 500\sin(\omega x)\cdot\sin(\omega y) \tag{17}$$

where $x \in L$ and L = 160, 80, 40, 20, 10 and 5 km, respectively. The basal bumps have a frequency of $\omega = 2\pi/L$. The bed topography and ice thickness are shown in Figure 2. The resulting surface velocity and stress fields are shown in Figures 3, 4 and 5.

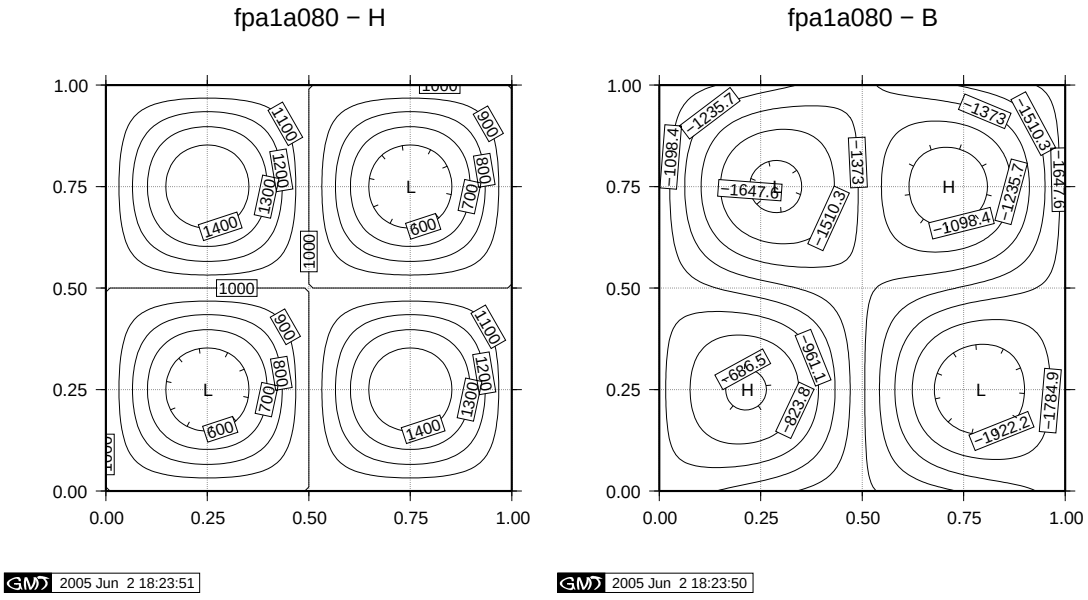

Figure 2: *Ice thickness and basal topography for experiment A with L = 80 km.*

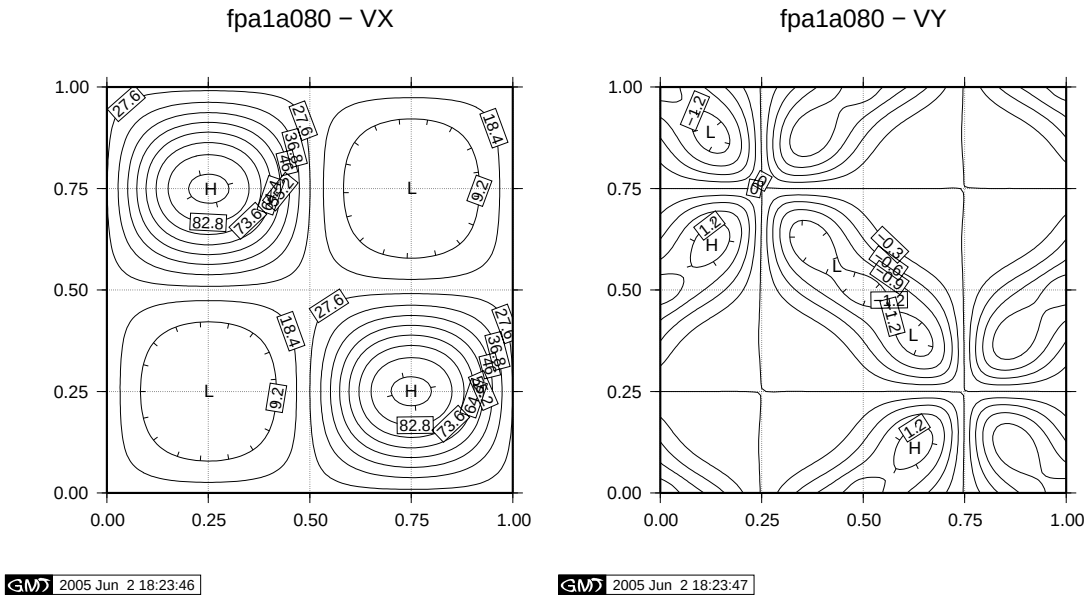

Figure 3: *Surface v_x and v_y velocity field for experiment A, obtained with a HHVF model for L = 80 km.*

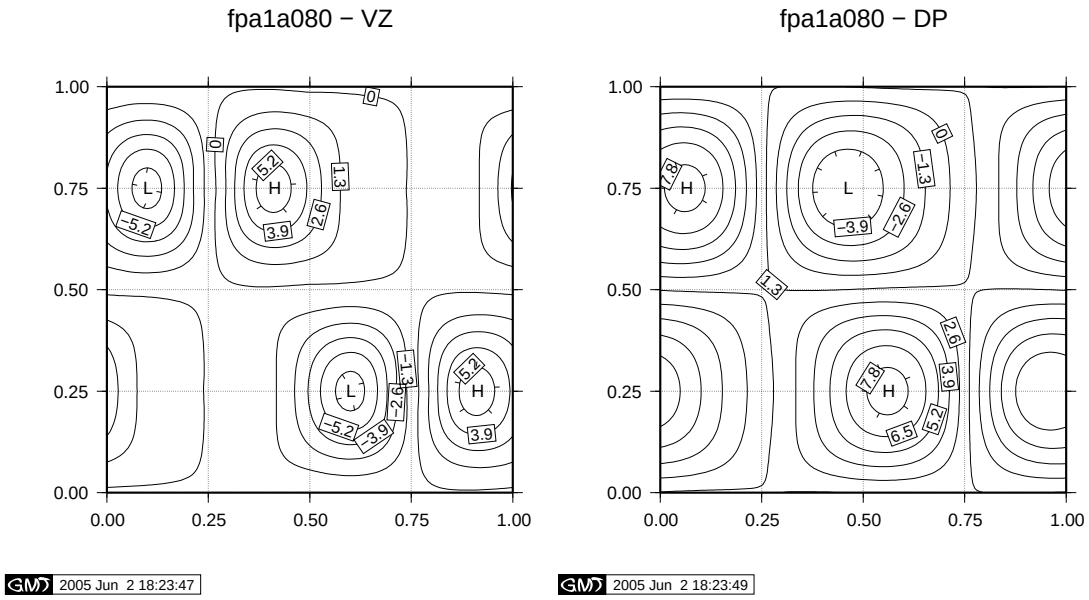

Figure 4: *Vertical velocity at the surface $v_z(z_s)$ and difference between the isotropic and hydrostatic pressure at the bed Δp for experiment A, obtained with a HHVF model for L = 80 km.*

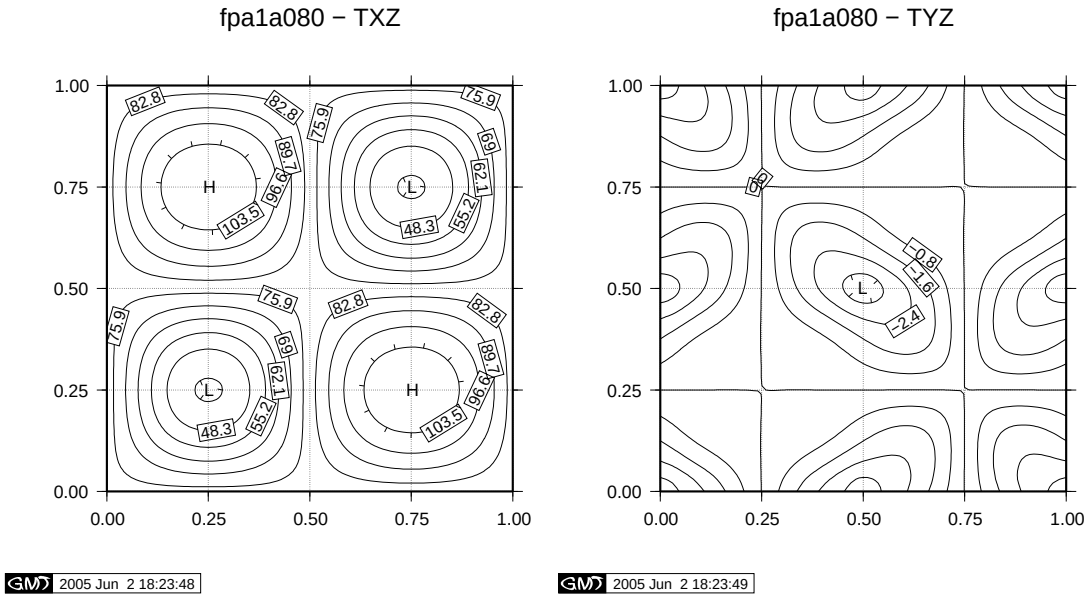

Figure 5: *Basal shear stresses* $\tau_{xz}(z_b)$ *and* $\tau_{yz}(z_b)$ *for experiment A, obtained with a HHVF model for* L *= 80 km.*

3.2 Experiment B: ice flow over a rippled bed

3.2.1 Type of models

HHVF, HHVC, HVF and HVC

3.2.2 Description of the experiment

The only difference with experiment A is that the basal topography does not vary with y, so that the experiment is suitable for 2D flowline models as well. The basal topography is thus formed by a series of ripples with an amplitude of 500 m.

$$z_s(x,y) = -x \cdot \tan\alpha \quad (18)$$

$$z_b(x,y) = z_s(x,y) - 1000 + 500\sin(\omega x) \quad (19)$$

where $x \in L$ and L = 160, 80, 40, 20, 10 and 5 km, respectively. The basal bumps have a frequency of $\omega = 2\pi/L$. Since the geometry of the experiment is designed for both HHV and HV models, the domain width is not important for HHV models (flowband). Flowline models do not consider any width variations along the flow line.

3.3 Experiment C: Ice stream flow I

3.3.1 Type of models

HHVF, HHVC and HHF

3.3.2 Description of the experiment

The experiment is similar to experiment A, albeit that the bedrock topography is flat, so that ice thickness remains constant for the whole domain (H = 1000 m).

$$z_s(x,y) = -x \cdot \tan\alpha \quad (20)$$

$$z_b(x,y) = z_s(x,y) - 1000 \quad (21)$$

where $x \in L$ and L = 160, 80, 40, 20, 10 and 5 km, respectively. Note that α takes a different value compared to the previous experiments, i.e. α = 0.1°! The basal friction coefficient is prescribed as

$$\beta^2(x,y) = 1000 + 1000 \sin(\omega x) \cdot \sin(\omega y) \quad (22)$$

The β^2-field is shown in Figure 6. The basal friction bumps have a frequency of $\omega = 2\pi/L$. A preview of the associated velocity and stress fields are shown in Figures 7, 8 and 9.

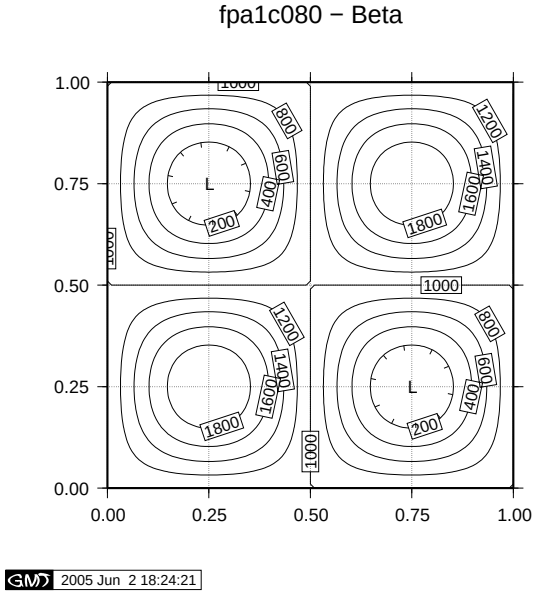

Figure 6: *Basal friction coefficient* β^2 *for experiment C with* L *= 80 km.*

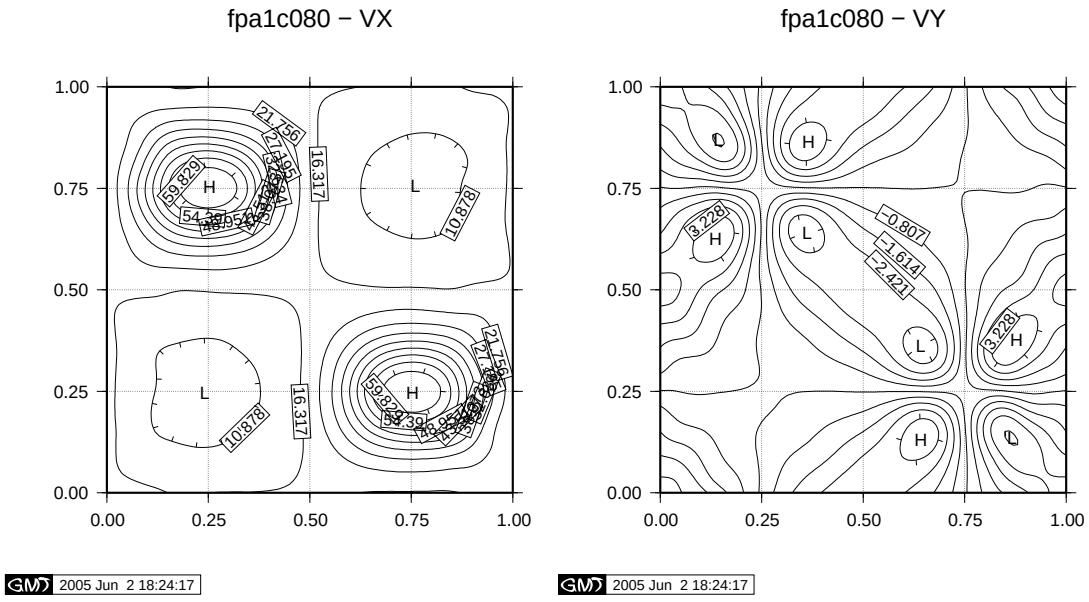

Figure 7: *Surface* v_x *and* v_y *velocity field for experiment C, obtained with a HHVF model for* L *= 80 km.*

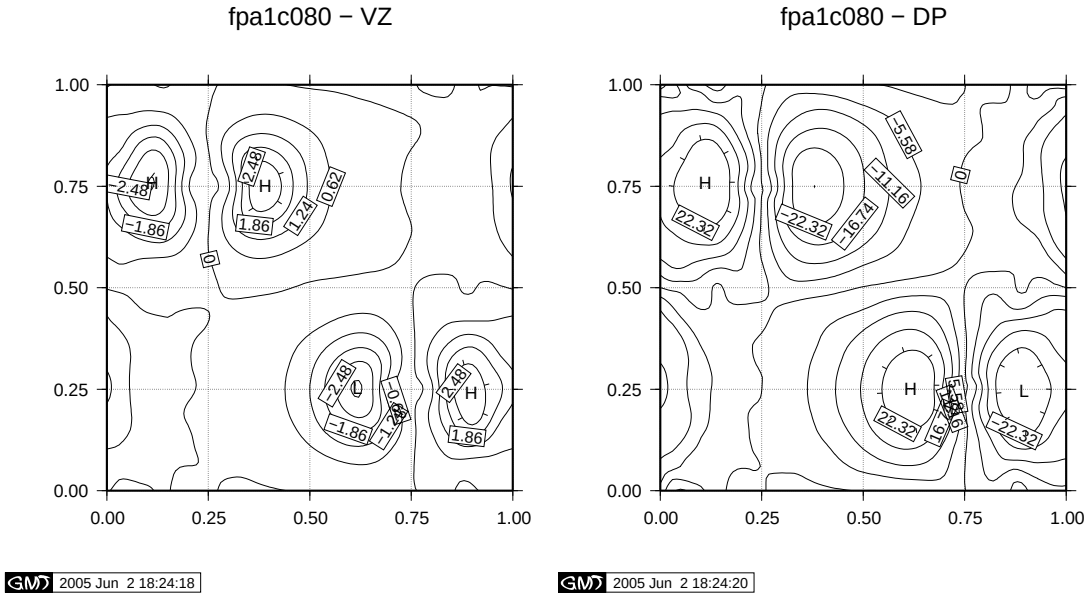

Figure 8: *Vertical velocity at the surface $v_z(z_s)$ and difference between the isotropic and hydrostatic pressure at the bed Δp for experiment C, obtained with a HHVF model for L = 80 km.*

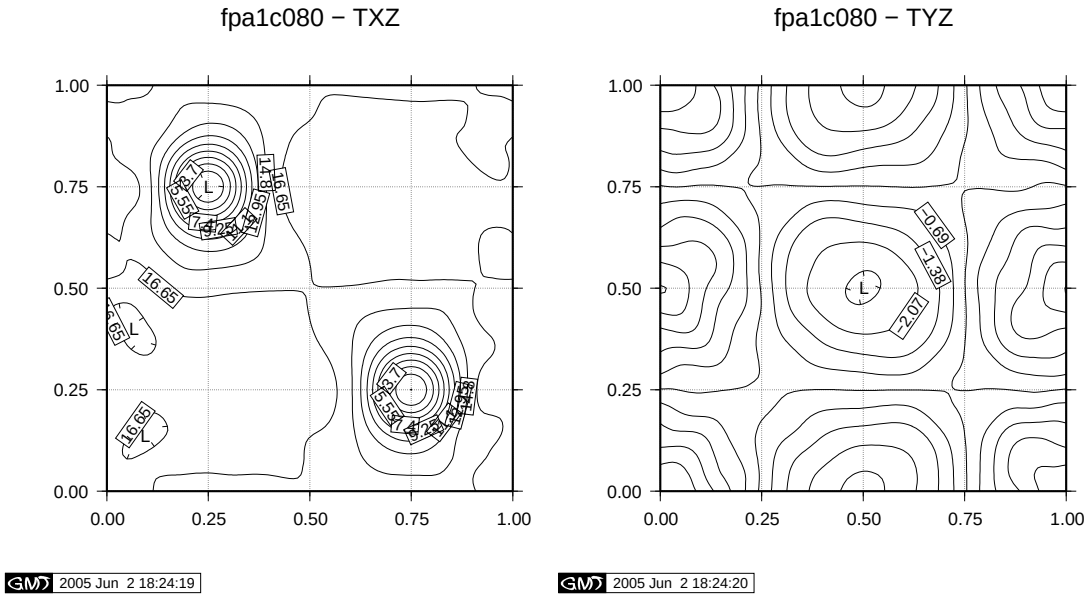

Figure 9: *Basal shear stresses $\tau_{xz}(z_b)$ and $\tau_{yz}(z_b)$ for experiment C, obtained with a HHVF model for L = 80 km.*

3.4 Experiment D: ice stream flow II

3.4.1 Type of models

HHVF, HHVC, HHF, HVF and HVC

3.4.2 Description of the experiment

The only difference with experiment C is that the basal friction coefficient does not vary with y, so that the experiment is suitable for 2D flowline models as well. The basal friction field is thus formed by a series of ripples defined as

$$\beta^2(x,y) = 1000 + 1000\sin(\omega x) \tag{23}$$

where the basal friction bumps have a frequency of $\omega = 2\pi/L$. Since the geometry of the experiment is designed for both HHV and HV models, the domain width is not important for HHV models (flowband). Flowline models do not consider any width variations along the flow line.

3.5 Experiment E: long profile of Haut Glacier d'Arolla

3.5.1 Type of models

HVF and HVC

3.5.2 Description of the experiment

Experiment E is a diagnostic experiment along the central flowline of a temperate glacier in the European Alps (Haut Glacier d'Arolla). The basic experiment and geometry is described in Blatter and others (1998) and Pattyn (2002).

Input for the model is formed by the longitudinal surface and bedrock profiles of Haut Glacier d'Arolla, Switzerland (Figure 10A). The longitudinal profile of this glacier has a very simple geometry, hence the resulting stress field is not influenced by geometrical perturbations such as the presence of a steep ice fall. In a first experiment, a zero basal velocity is considered ($\beta^2 = \infty$), and the width of the drainage basin, is kept equal to 1 along the whole flowline domain, so that HVC and HVF models should give similar results. The flow-law rate factor A is taken constant over the whole model domain, and equals A = 10^{-16} Pa^{-n} a^{-1}. Upstream and downstream boundary conditions imply a zero ice thickness and zero ice velocity. The horizontal grid resolution is taken as $\Delta x =$ 100 m.

A second experiment considers a narrow zone of zero traction, similar to the experiment described in Blatter and others (1998):

$$\begin{aligned} \beta^2 &= 0 \qquad \text{for} \quad 2200 \leq x \leq 2500\text{m} \\ \beta^2 &= +\infty \qquad \text{otherwise} \end{aligned}$$

The zero traction zone therefore extends over four grid points, i.e. from $i = 23$ to $i = 26$. The input 'arolla100.dat' file consist of four columns with x [m] in the first, z_s [m] in the second, z_b in the third column, and the value 0 or 1 in the fourth, where 1 denotes the zone of zero basal friction. The number of grid points totals 51.

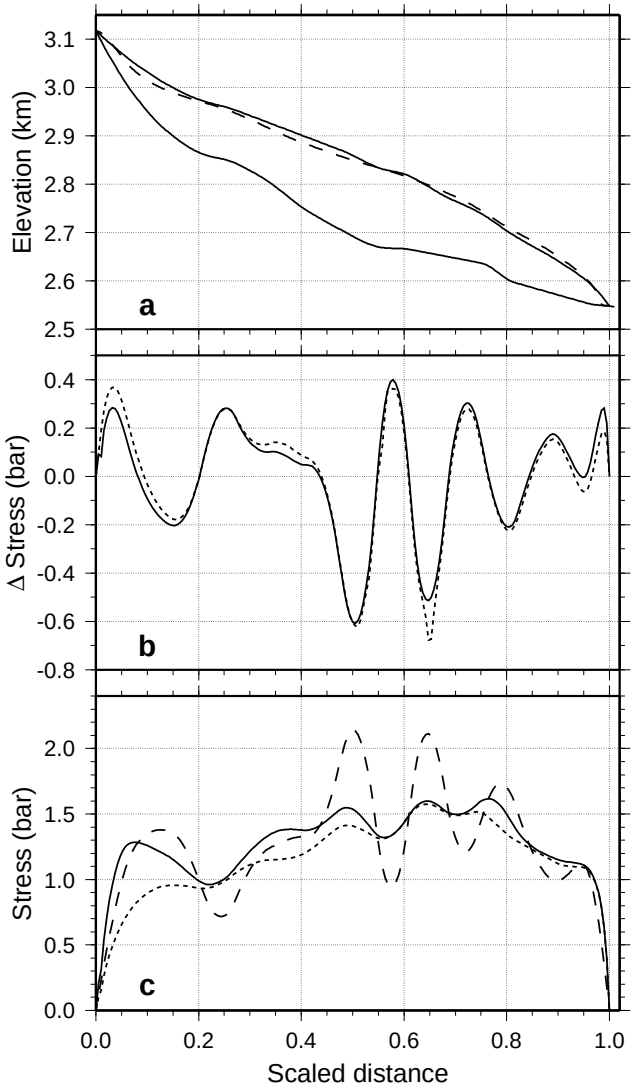

Figure 10: *(a) Longitudinal profile of Haut Glacier d'Arolla, taken from Blatter and others (1998) (solid line); (b) the difference between the basal drag and the driving stress* $\tau_b - \tau_d$ *(solid line) versus the vertically-integrated longitudinal stress gradient* $2\frac{\partial}{\partial x}(H\overline{\tau}_{xx})$ *(dotted line); (c) basal drag* τ_b *(solid line), basal shear stress* $\tau_{xz}(z_b)$ *(dotted line) and driving stress* τ_d *(dashed line). The horizontal model resolution is 20 m (taken from Pattyn, 2002).*

3.6 Experiment F: prognostic experiment for a linearly viscous medium

3.6.1 Type of models

HHVF and HHVC

3.6.2 Description of the experiment

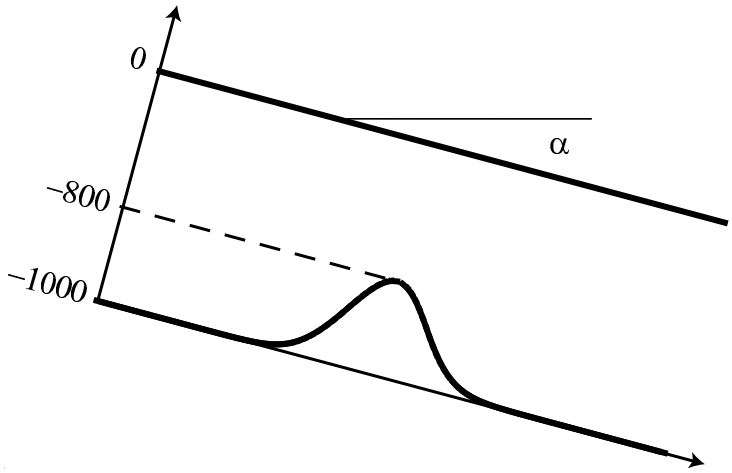

Figure 11: *Coordinate system for experiment F.*

Experiment F is a prognostic experiment for which the free surface is allowed to relax until a steady state is reached for a zero surface mass balance:

$$\lim_{t\to\infty}\frac{\partial H}{\partial t}=\lim_{t\to\infty}\left[-\nabla\int_{z_b}^{z_s}\vec{\mathbf{v}}\mathrm{d}z\right]=\lim_{t\to\infty}\left[-\nabla(\overline{\vec{\mathbf{v}}}H)\right]=0\,, \tag{24}$$

where $\vec{\mathbf{v}}$ is the horizontal velocity vector (m a^{-1}) and H is the ice thickness (m). Consider a parallel-sided slab of ice lying on a sloping bed (Figure 1) with a mean slope α = 3.0°. The slope is zero in the y direction and maximal in the x direction. Basic model setup differs from the setup in experiments A and C by:

1. A slab of ice with mean ice thickness $H^{(0)}$ = 1000 m is considered, resting on a sloping bed with a mean slope of α = 3.0°. This slope is maximum in x and zero in y. The bedrock plane is parallel to the surface plane and perturbed by a Gaussian bump. Initial bedrock $B^{(0)}$ and unperturbed surface $S^{(0)}$ elevation are thus governed by

$$S^{(0)}(x,y) = 0 \tag{25}$$

$$B^{(0)}(x,y) = -H^{(0)} + a_0 \left(\exp\left[\frac{-(x^2+y^2)}{\sigma^2} \right] \right) \tag{26}$$

where $\sigma = 10000 = 10H^{(0)}$ and where x,y (m) is the distance to the center of the domain that has the coordinates (0, 0). The basal perturbation has a maximum height of one tenth of the mean ice thickness, i.e. $a_0 = 100 = 0.1H^{(0)}$ (Figure 12).

2. The domain size L is at least 100 $H^{(0)}$ in x and y. The horizontal coordinates for output are scaled against σ by

$$\hat{x} = \frac{x}{H^{(0)}} \qquad \hat{y} = \frac{y}{H^{(0)}} \tag{27}$$

3. Periodic boundary conditions can be applied as is the case in experiment A, but this is not at all necessary when the domain is taken large enough

4. n = 1 in (6), so that the effective viscosity in (7) reads $\eta = \frac{1}{2A}$ and is a constant.

5. The unperturbed velocity field at the surface is defined by

$$U^{(0)} = AH^{(0)}\tau_b^{(0)} = \rho g A \left[H^{(0)} \right]^2 \sin\alpha \tag{28}$$

where $\tau_b^{(0)} = \rho g H^{(0)} \sin\alpha$ is the unperturbed basal shear stress, and A = 2.140373 $\times$ 10^{-7} Pa^{-1} a^{-1}, so that $U^{(0)}$ = 100 m a^{-1}.

6. Experiments are carried out for different values for slip ratios c, that determine the relation between the basal velocity and basal drag. As seen in 2.1.2, the basal velocity is written in terms of a basal friction coefficient β^2, or

$$U_b = \frac{\tau_b}{\beta^2} \tag{29}$$

Following the scalings given by Gudmundsson (2003), the basal friction coefficient is related to the slip ratio c by:

$$\beta^2 = \left(cAH^{(0)} \right)^{-1} \tag{30}$$

Experiments are run for slip ratios c = 0 and 1. It is easily demonstrated that $U_b^{(0)} = cU^{(0)}$.

Table III lists the main constants used for experiment F. Using these settings, the model should run until a steady state of the free surface is reached. The output is the surface velocity field (all three components) and the relaxed surface elevation. Figures 13 and 14 show the steady state surface elevation and surface velocity fields for the experiment with c = 0.

Symbol	Constant	Value	Units
A	Ice-flow parameter	2.140373×10^{-7}	$Pa^{-1}\ a^{-1}$
n	Flow law exponent	1	
α	Mean surface slope	3°	
a_0	Amplitude Gaussian bump	100	m
σ	Width Gaussian bump	10000	m

Table III: *Constants for the model setup according to experiment F.*

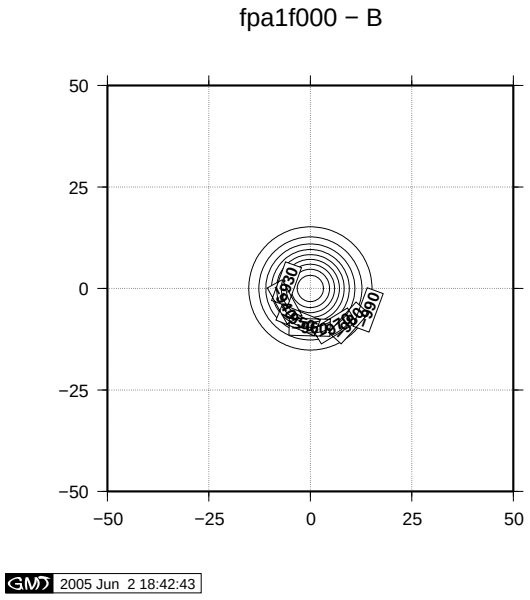

Figure 12: *Bed topography for experiment F.*

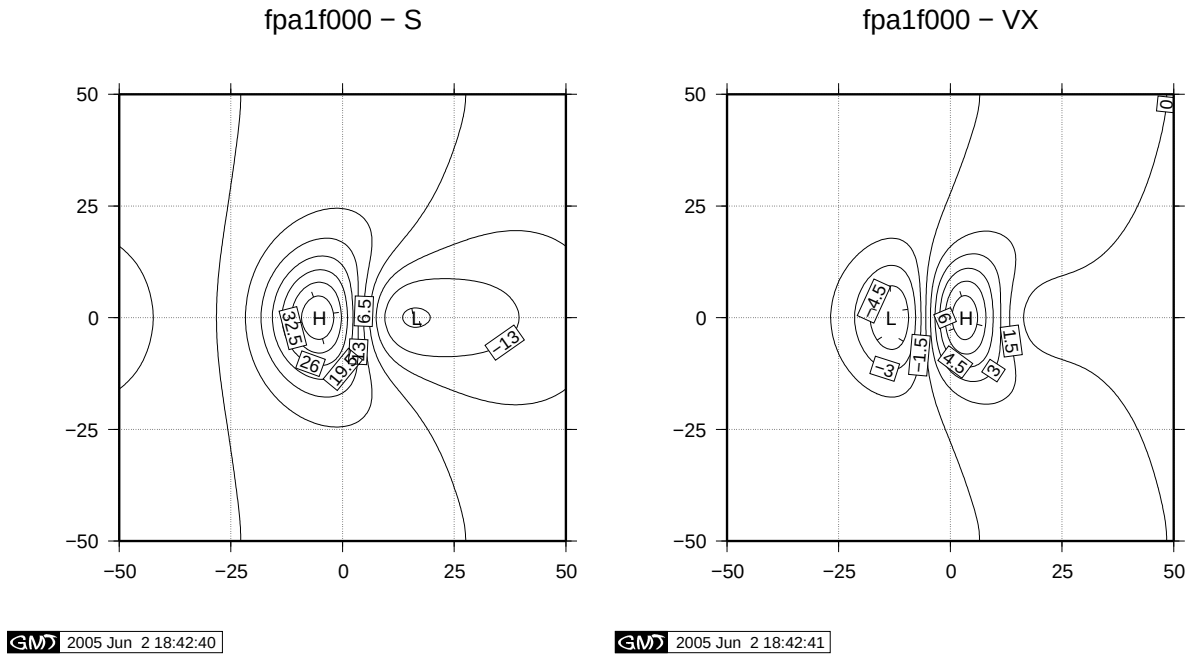

Figure 13: *Perturbed steady state surface elevation S and surface velocity v_x for experiment F with c = 0.*

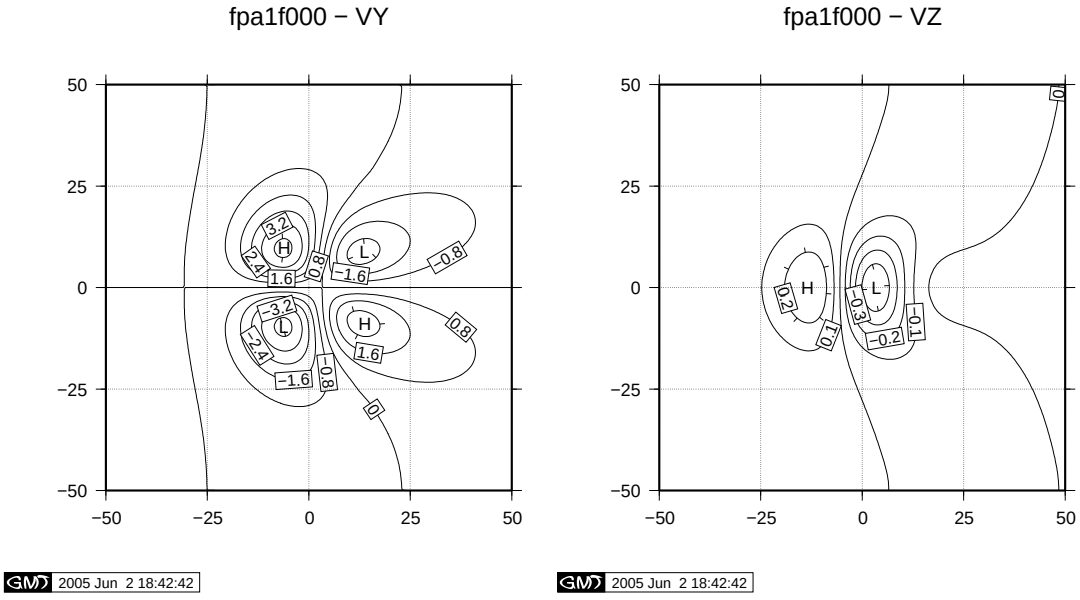

Figure 14: *Perturbed steady state surface velocity v_y and v_z for experiment F with c = 0.*

4 Model output

Output is produced for all gridpoints in the horizontal plane that were used in the model calculation for the domain lying between 0 and L (or between 0 and 1 for the scaled coordinates) in both horizontal directions. All variables are taken either at the surface z_s or at the bottom z_b.

4.1 Experiment A

For experiment A, the following output must be produced for each grid point of the modeled domain. The number of lines will depend on the grid resolution used. The total number of columns equals 8:

$\hat{x}$	$\hat{y}$	$v_x(z_s)$	$v_y(z_s)$	$v_z(z_s)$	$\tau_{xz}(z_b)$	$\tau_{yz}(z_b)$	Δp

where units are m a^{-1} for velocity and kPa for stress and pressure.

4.2 Experiment B

For experiment B, the following output must be produced for each grid point of the modeled domain along the flowline (for flowline models) or along the central line in y for 3D models. The number of lines will depend on the grid resolution used. The total number of columns equals 5:

$\hat{x}$	$v_x(z_s)$	$v_z(z_s)$	$\tau_{xz}(z_b)$	Δp

where units are m a^{-1} for velocity and kPa for stress and pressure.

4.3 Experiment C

For experiment C, the following output must be produced for each grid point of the modeled domain. The number of lines will depend on the grid resolution used. The total number of columns equals 10:

$\hat{x}$	$\hat{y}$	$v_x(z_s)$	$v_y(z_s)$	$v_z(z_s)$	$v_x(z_b)$	$v_y(z_b)$	$\tau_{xz}(z_b)$	$\tau_{yz}(z_b)$	Δp

where units are m a^{-1} for velocity and kPa for stress and pressure.

4.4 Experiment D

For experiment D, the following output must be produced for each grid point of the modeled domain along the flowline (for flowline models) or along the central line in y for 3D models. The number of lines will depend on the grid resolution used. The total number of columns equals 6:

$\hat{x}$	$v_x(z_s)$	$v_z(z_s)$	$v_x(z_b)$	$\tau_{xz}(z_b)$	Δp

where units are m a^{-1} for velocity and kPa for stress and pressure.

4.5 Experiment E

For experiment E, the following output must be produced for each grid point of the modeled domain along the flowline. The number of lines equals 51. The total number of columns equals 5:

$\hat{x}$	$v_x(z_s)$	$v_z(z_s)$	$\tau_{xz}(z_b)$	Δp

where units are m a^{-1} for velocity and kPa for stress and pressure.

4.6 Experiment F

For experiment F, the following output must be produced for each grid point of the surface of the modeled domain. The number of lines will depend on the grid resolution used. The total number of columns equals 6:

$\hat{x}$	$\hat{y}$	z_s	v_x	v_y	v_z

Please note that these variables refer to the perturbed steady state solution.

4.7 Output and file format

Output should be written in a (by preference tabulated) ASCII text file. The file name should look as follows:

NNNMELLL.txt

where

NNN = three letter code of your name (first character of first name followed by the two first characters of your last name, e.g. ‘fpa’ for Frank Pattyn or ‘tpa’ for Tony Payne)

M = model number, equals 1 if you submit results of only one model or type of model.

E = Experiment number: a, b, c, d, or e

LLL = three numbers denoting the length L (km) of the domain, i.e. 160, 080, 040, 020, 010, or 005. For experiment E, this becomes 000 for the standard non-sliding experiment and 001 for the experiment with the zone of zero basal traction. For experiment F, this denotes the slip ratio, i.e. 000 or 001.

It is advised to refrain from the use of capital characters in the name of the experiment files. For example, the file named fpa1c016.txt contains the results of experiment C for a length scale L = 16 km with model number 1 of Frank Pattyn. The file must contain 10 columns.

A separate pdf file or word document with the name NNNmodel.pdf or NNNmodel.doc (e.g. fpamodel.pdf) should contain a detailed description of the used model(s), clearly indicating which model corresponds to which model number. Please give ample information and references on the type of model and the stress components involved.

REFERENCES

Blatter, H., G. Clarke, and J. Colinge. 1998. Stress and velocity fields in glaciers: Part II. sliding and basal stress distribution. *J. Glaciol.*, **44**(148), 457–466.

Gudmundsson, G. 2003. Transmission of basal variability to a glacier surface. *J. Geophys. Res*, **108**(B5, 2253), doi:10.1029/2002JB002107.

Hindmarsh, R. 2004. A numerical comparison of approximations to the Stokes equations used in ice sheet and glacier modeling. *J. Geophys. Res*, **109**(F01012), doi:10.1029/2003JF000065.

MacAyeal, D. 1993. A tutorial on the use of control methods in ice-sheet modeling. *J. Glaciol.*, **39**(131), 91–98.

Pattyn, F. 2002. Transient glacier response with a higher-order numerical ice-flow model. *J. Glaciol.*, **48**(162), 467–477.

Pattyn, F. 2003. A new 3D higher-order thermomechanical ice-sheet model: Basic sensitivity, ice-stream development and ice flow across subglacial lakes. *J. Geophys. Res.*, **108**(B8, 2382), doi:10.1029/2002JB002329.